Circulation Journal
Official Journal of the Japanese Circulation Society
http://www.j-circ.or.jp

Supplemental File
*Circ J* 20XX; **XX:** XXX–XXX

# Triggered Firing and Atrial Fibrillation in Transgenic Mice With Selective Atrial Fibrosis Induced by Overexpression of TGF-$\beta$1

Eue-Keun Choi, MD, PhD; Po-Cheng Chang, MD; Young-Soo Lee, MD, PhD; Shien-Fong Lin, PhD; Wuqiang Zhu, MD, PhD; Mitsunori Maruyama, MD, PhD; Michael C. Fishbein, MD; Zhenhui Chen, PhD; Michael Rubart-von der Lohe, MD; Loren J. Field, PhD; Peng-Sheng Chen, MD

## Supplemental File 1

Please provide title.

### Data S1. ??????

### Method

#### Experimental Preparations

MHC-TGFcys$^{33}$ser mice express a human transforming growth factor $\beta$1 (TGF-$\beta$1) cDNA (harboring a cystein-to-serine substitution at amino acid residue 33) under the regulation of the cardiac-restricted $\alpha$-cardiac myosin heavy chain promoter. The cys$^{33}$ser substitution blocks tethering of the small latent complex to LTBP-1, thereby resulting in elevated activity.[S1] We used 18 transgenic (Tx)[S2] and 18 wild-type (Wt) mice for simultaneous optical mapping of membrane potential (Vm) and intracellular $Ca^{2+}$ ($Ca_i$) transient; 6 Tx and 6 Wt mice were used for the histological analyses. An additional 6 Wt mice were used to determine the effects of extracellular $Ca^{2+}$ concentration on action potential duration (APD). The mean age of the Tx and Wt mice was 142±33 days (range 88–196 days) and 171±41 days (range 88–222 days), respectively. The research protocol was approved by the Institutional Animal Care and Use Committee and conforms to the guidelines of the American Heart Association.

After intraperitoneal injection of heparin (0.5 U/g), mice were killed by cervical dislocation. The hearts were rapidly excised and rinsed in iced Tyrode's solution (in mmol/L: NaCl 125, KCl 4.5, $NaH_2PO_4$ 1.8, $NaHCO_3$ 24, $CaCl_2$ 0.9, $MgCl_2$ 0.5, and glucose 5.5 in deionized water with pH equilibrated to 7.4±0.5). The ascending aorta was immediately cannulated and the hearts were perfused retrogradely with a Langendorff perfusion system with warm oxygenated Tyrode's solution (37°C, 95% $O_2$, 5% $CO_2$) at a constant pressure of 70–80 mmHg (flow rate 1–2 ml/min). The hearts were immersed in the temperature-controlled tissue bath and maintained at 37°C. Pseudo-ECG recording was obtained utilizing the bath solution as a volume conductor. The calcium indicator Rhod-2-acetoxymethyl ester (5 $\mu$mol/L, Molecular Probes, Eugene, OR, USA, dissolved in dimethyl sulfoxide via mixing with pluronic F-127) was loaded for 30-min period. The voltage indicator Rh-237 (Molecular Probes) was administered as a bolus through a side-port in the perfusion system. After staining, the ventricles were removed beneath the atrioventricular ring. The atria were removed under microscopic guidance and superfused with the Tyrode solution.[S3] Blebbistatin (5 $\mu$mol/L) was added to the Tyrode's solution for immobilization of the preparation. This concentration was lower than that used in previous studies by others,[S4,S5] but was sufficient to reduce motion artifacts given the low external $Ca^{2+}$ concentration used in dual optical mapping experiments. We used 10 $\mu$mol/L blebbistatin in 6 experiments designed to test the effects of extracellular $Ca^{2+}$ concentration on APD. The temperature was maintained at 37±0.5°C. The isolated atria were illuminated with a solid-state, frequency-doubled laser (Verdi, Coherent Inc, Santa Clara, CA, USA) at a wavelength of 532 nm. The emitted fluorescence was filtered through a 580±20 nm bandpass filter for the $Ca_i$ signal recording and a 715-nm long-pass filter for Vm recording. The fluorescence was then acquired simultaneously with 2 high-speed cameras (MiCAM Ultima, BrainVision, Tokyo, Japan) at 0.5 ms/frame. The digital images (100×100 pixels) were gathered from both atria in a 7×7 mm$^2$ area, resulting in a pixel resolution of 70×70 $\mu$m$^2$ per pixel.

#### Experimental Protocol

In the first 18 mice studied, atrial conduction properties were measured during rapid atrial pacing from the lower interatrial septum at a pacing cycle length (PCL) of 150, 130, 100, and 70 ms. Electrical stimulation was delivered with 1.5× diastolic capture threshold using World Precision Instrument model A385R constant current isolator (Sarasota, FL, USA). If atrial tachycardia (AT) or atrial fibrillation (AF) was induced, we waited for a minimum of 2 min after termination before the next pacing attempt. This sequence of burst pacing was repeated once. If 1 or more bursts in the 2 series of bursts evoked an AF episode, AF was considered to be inducible in that animal; otherwise, AF was considered to be noninducible. Following completion of the pacing protocol, the hearts were superfused with Tyrode's solution containing carbachol (carbamylcholine, 1–3 $\mu$mol/L; Sigma, St. Louis, MO, USA). The carbachol dosage was increased until there was a 25% decrease in heart rate.[S6] The same programmed stimulation protocol was then used to induce AF. After the baseline and carbachol studies, ryanodine (3 $\mu$mol/L) and thapsigargin (1 $\mu$mol/L) were added to the perfusate for 30 min and the same pacing protocol was repeated.

To determine the effects of external $Ca^{2+}$ concentration on APD, we studied isolated atria from 6 additional Wt mice. After staining with 10 ml of Di-4 APPNES (2.5 $\mu$mol/L), the atria were isolated and superfused with Tyrode's solution containing 10 $\mu$mol/L blebbistatin and 1.8 mmol/L $CaCl_2$. The preparation was paced at 150 ms for 1 h and optical mapping was performed to determine the APD. We then reduced $CaCl_2$ to 0.9 mmol/L and repeated the optical mapping 20 min later at the same PCL.

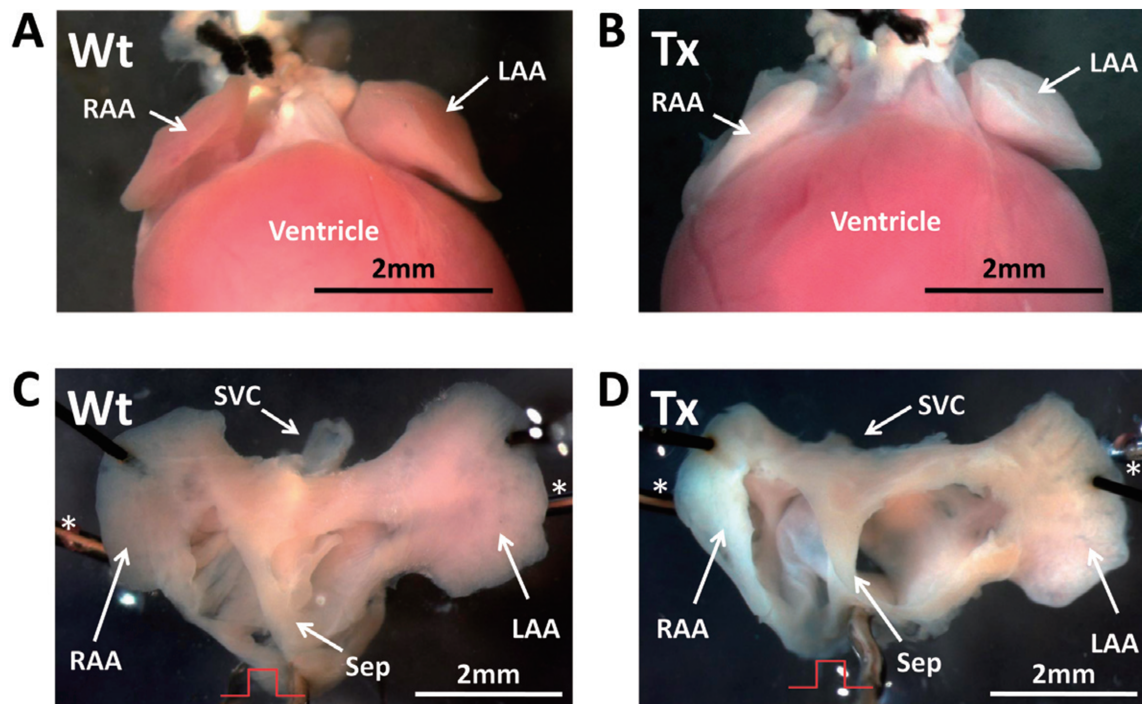


**Figure S1.** Photograph of a typical preparation of isolated mouse atrium, showing the positioning of the electrogram and stimulus. The right atrium is to the left of image. (**A**) Wild-type (Wt) and (**B**) transgenic (Tx) hearts. (**C**,**D**) In vitro isolated atrial preparation of the same hearts. The atria of the Tx mice are more white than the Wt atria in both the intact heart preparation (**A**,**B**) and the isolated atrium preparation (**C**,**D**). RAA, right atrial appendage; LAA, left atrial appendage; Sep, septum; SVC, superior vena cave; the ohm symbol is the site of pacing; *electrode for pseudo-ECG.

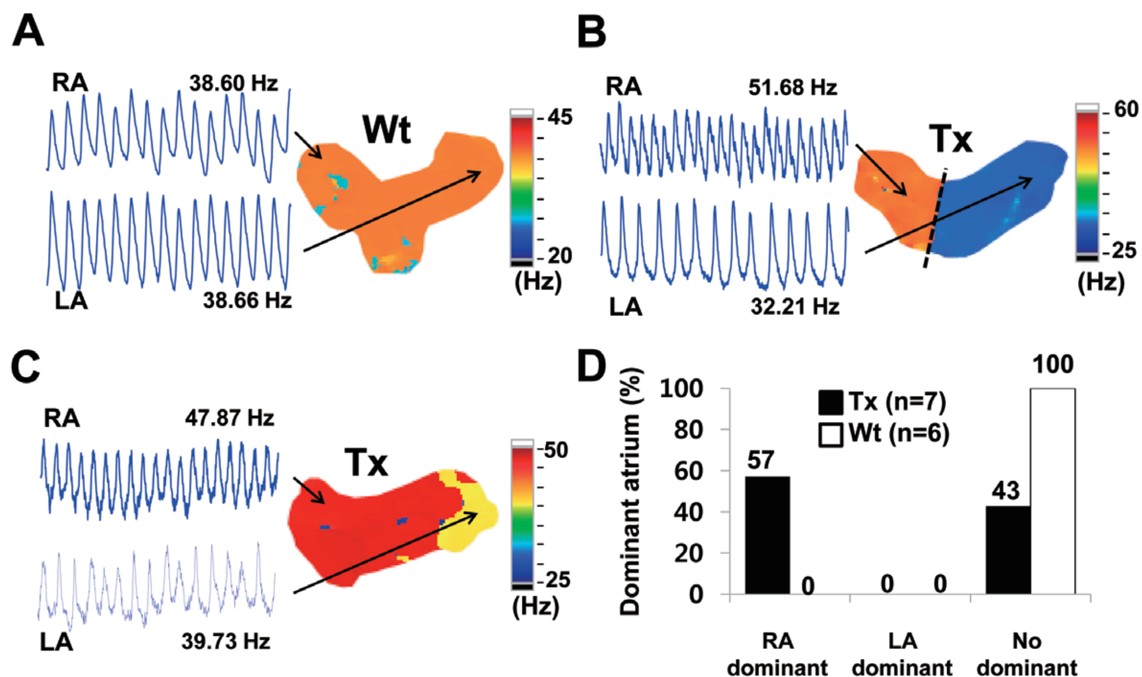


**Figure S2.** Dominant frequency (DF) map during atrial fibrillation (AF) in wild-type (Wt) and transgenic (Tx) mice. Wt mice show a similar DF in the right (RA) and left (LA) atria (**A**). More than half of the Tx mice show a RA-dominant pattern on the DF map (**B**), whereas 43% show no difference (**C**). (**D**) Summary of DF map according to Tx and Wt mice.

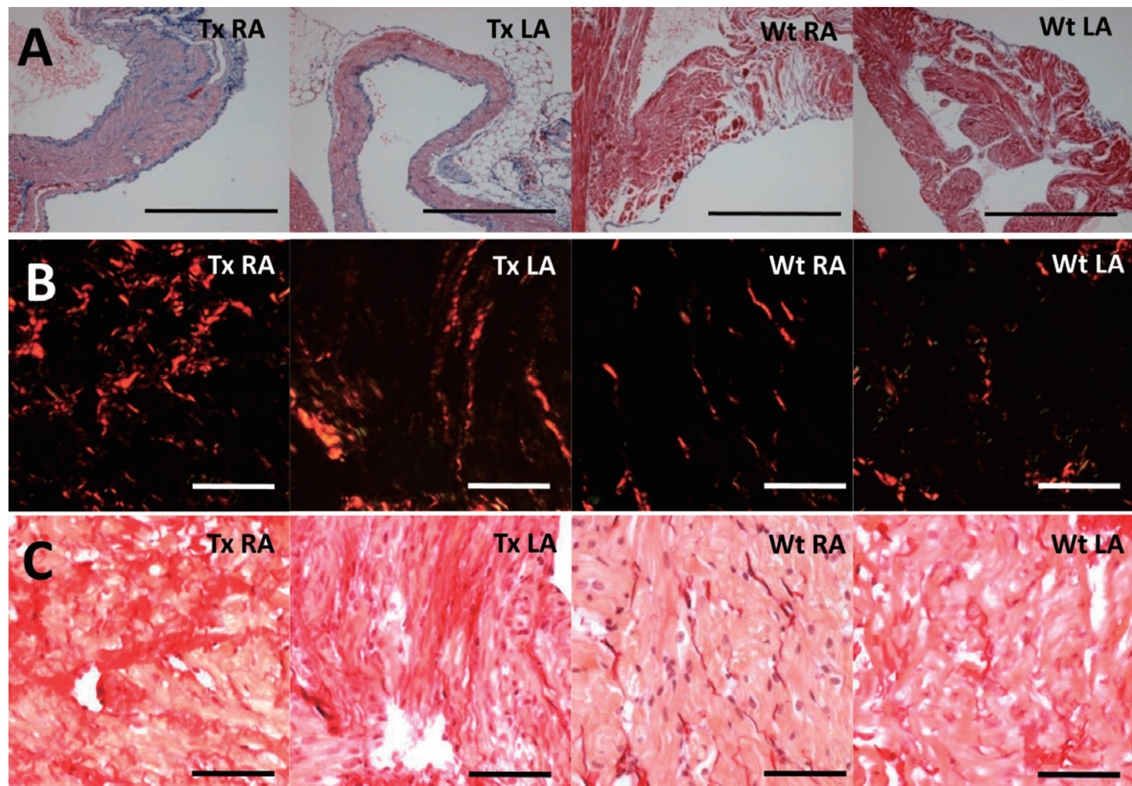


**Figure S3.** Histological findings. (**A**) Trichrome staining in which myocytes are stained red and fibrotic tissue is stained blue. The atria of transgenic (Tx) mice stained purple while the wild-type (Wt) atria stained red, indicating increased fibrosis in the Tx atria. (**B**) Picrosirius red staining examined under polarized light and (**C**) shows the same stain under light microscope. There was more fibrosis in Tx atria than in Wt atria. Moreover, the Tx-RA had more fibrosis than the Tx-LA. Calibration bars are 1 mm in (**A**) and 50 $\mu$m in (**B**,**C**). LA, left atrium; RA, right atrium.

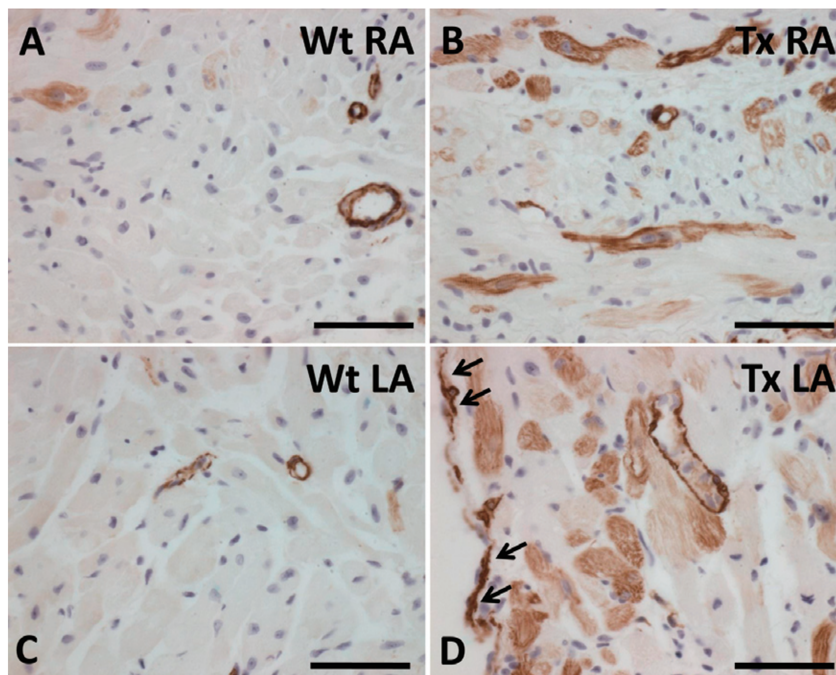


**Figure S4.** Histological evaluation of transgenic (Tx) and wild-type (Wt) atria. Alpha-smooth-muscle actin ($\alpha$-SMA) immune reactivity shows increased density of myofibroblasts (black arrows) and $\alpha$-SMA induction in cardiomyocytes in Tx mice (**B**,**D**) compared with Wt mice (**A**,**C**). Calibration bars are 50 $\mu$m.

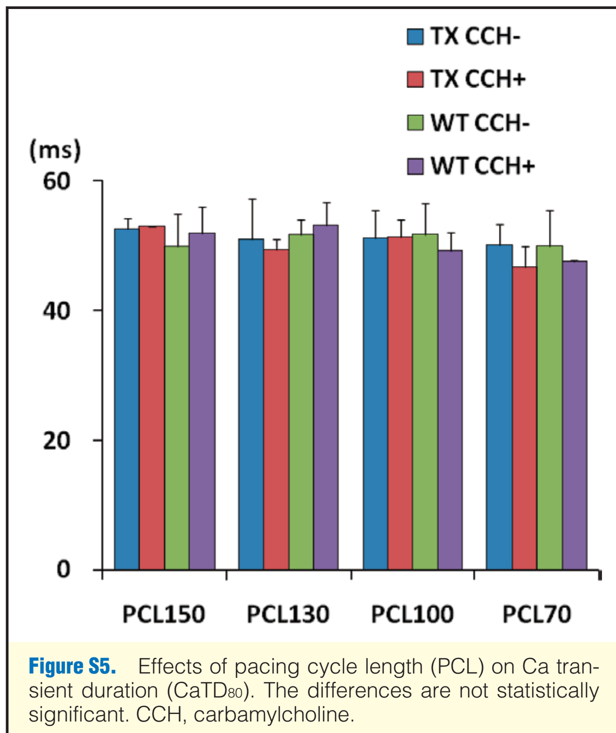


**Figure S5.** Effects of pacing cycle length (PCL) on Ca transient duration ($CaTD_{80}$). The differences are not statistically significant. CCH, carbamylcholine.

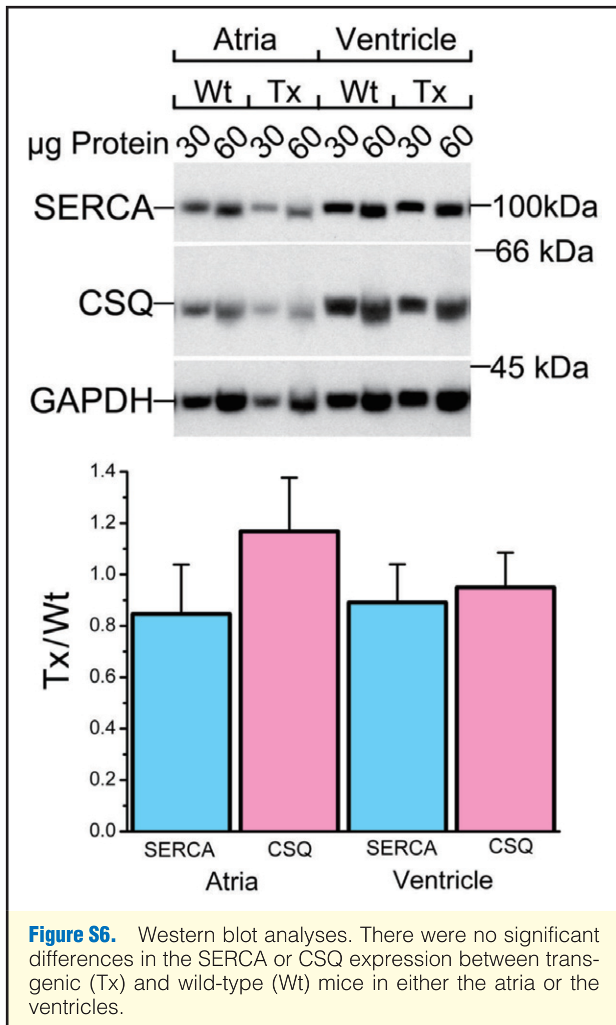


**Figure S6.** Western blot analyses. There were no significant differences in the SERCA or CSQ expression between transgenic (Tx) and wild-type (Wt) mice in either the atria or the ventricles.

## Histology

Whole preparations were fixed in 4% formalin for 45–60 min, followed by immersion in 70% alcohol. The tissues were then paraffin embedded and cut into 5-$\mu$m thick sections. The slides were then stained with picrosirius red and examined under polarized light. The digital pictures were then used to calculate the percent of fibrosis. Subendocardial and subepicardial connective tissues were excluded from analyses. A monoclonal antibody to $\alpha$-smooth-muscle actin (SMA; DAKO, CA, USA) was used to stain activated myofibroblasts, smooth muscle cells and dedifferentiated myocytes.[S7] The percent of area of positive $\alpha$-SMA was calculated using custom-developed software.

## Western Blot Analyses

In total, 5 Tx and 5 Wt mice were killed and their hearts were harvested for western blot analyses. Of the homogenates of atrial or ventricular tissue, 30 $\mu$g and 60 $\mu$g, respectively, were loaded onto 8% polyacrylamide SDS-PAGE and transferred to a nitrocellulose membrane. The blot was probed with the monoclonal anti-sarco/endoplasmic reticulum $Ca^{2+}$-ATPase 2a (SERCA2a) antibody, 2A7-A1, a polyclonal anti-calsequestrin (CSQ) antibody, and a monoclonal anti-glyceraldehydes-3-phosphate-dehydrogenase (GAPDH) antibody (Peirce). Antibody-binding protein bands were visualized by $^{125}$I-protein A and quantified with a Bio-Rad Personal Fx phosphorimager.

## Data Analysis

APD was measured from 20% depolarization to 80% repolarization ($APD_{80}$) at a PCL of 150 ms. We measured 2 points from the right atrial (RA) appendage and 2 points from the RA septum, and then averaged the 4 points for the RA $APD_{80}$. The left atrial (LA) $APD_{80}$ was calculated by the same method (2 from the LA appendage and 2 from the LA septum). $Ca_i$ transient $duration_{80}$ ($Ca_iTD_{80}$) was measured by the same method. Conduction velocity was calculated using the distance between the pacing site and the end of the tip of each atrial appendage and the time interval between commencement of pacing and when the entire atrial preparation was activated. Focal discharge was defined as an activation wavefront that propagated in all directions on the optical maps. AT was defined as tachycardia with regular intervals on the pseudo-ECG and a single focus of activation on the corresponding optical maps. AF is defined as tachycardia with irregular intervals on the pseudo-ECG, because of multiple foci of activation, alternating foci of activation or the coexistence of multiple reentrant wavefronts. Fast-Fourier transform was used to determine the frequency at each pixel during AF. The dominant frequency (DF) maps were plotted using the DF of activation at different mapped regions. We defined the dominant atrium as the 1 having a DF value that was at least 10 Hz higher than that of the other atrium. If the difference in maximum DF between the RA and LA was less than 10 Hz, neither atrium was deemed dominant. Phase maps were constructed with a time-delay embedding method.[S8] Phase singularity was defined as a site with an ambiguous phase with its neighboring pixels exhibiting a continuous progression of phase from $-\pi$ (pi) to $+\pi$ (pi).[S9] The cumulative phase-singularity map was constructed by plotting the phase singularities of 100 consecutive frames (50 ms) on the same map to determine the spatial dispersion of the phase singularities.[S10]

Continuous variables are expressed as the means ± SD, and discrete variables are presented as absolute values and percentages. Student's t-test was used to analyze continuous variables and the chi-square test or Fisher's exact test was used for categorical variables.

## Results

Compared with Wt atria, the atria of the Tx mice were whiter, consistent with increased fibrosis (**Figure S1**).

### DF During AF

We analyzed the DF during AF in Tx (n=7) and Wt atria (n=6). There were no significant differences in DF between the 2 groups (63.2±24.7 Hz in Tx vs. 62.1±23.9 Hz in Wt atria, P>0.05). However, 4 of 7 Tx atria exhibited a RA-dominant pattern (ie, higher DF in the RA than in the LA). **Figure S2A** shows a typical example of the DF distribution in Wt atria. **Figure S2B** shows an example of the RA-dominant pattern in Tx atria, with the septum as a structure that separated the 2 different DF regions. It is possible that the septum in this case is acting as a propagation barrier. Alternatively, the difference in fibrosis between the 2 atria resulted in the differential DF. **Figure S2C** shows a Tx atria that failed to show a difference in DF between the RA and LA, although a small portion of the LA (to the right) had a lower DF than the rest of the atria. **Figure S2D** summarizes the results.

### Distribution of Atrial Fibrosis in Tx Atria

The morphology of the Tx hearts was normal and did not show atrial dilatation, consistent with that reported elsewhere.[S2,S11] **Figure S3** summarizes the histological findings. **Figure S3A** shows the trichrome staining of the Tx and Wt atria. We quantified the atrial fibrosis in 6 Tx and 6 Wt mice. In agreement with a previous report,[S2] the fibrotic area (as measured by visualization of picrosirius red stained sections under polarized light) of the RA was greater than that of the LA in Tx mice (27.1±2.6% vs. 18.7±2.6%, P=0.01), and both areas were greater than in the Wt RA and LA (3.6±0.6%, P=0.007 and 4.7±0.5%, P=0.007, respectively). The thickness of the atrial free wall in these preparations was invariably less than 1 mm. The $\alpha$-SMA immunostaining reactivity was used to screen for the presence of myofibroblasts (**Figure S4**). The area with $\alpha$-SMA-positive cells was greater in Tx atria than in Wt atria (23.1±7.1% in the Tx vs. 1.9±0.9% in the Wt, P<0.001). The areas with $\alpha$-SMA positivity in the LA and RA were not significantly different (26.6±7.5% in the Tx-LA vs. 19.7±5.4% in the Tx RA, P>0.05). An unexpected finding was the presence of scattered $\alpha$-SMA-positive myocytes in both atria.

Interestingly, the DF was also more prominent in the RA than in the LA, providing additional evidence (albeit circumstantial) for a causal relationship between the degree of fibrosis and electrophysiological changes/arrhythmia susceptibility. In addition, we demonstrated that most of the triggered activities and all of the first and second beats after spontaneous AF reinitiation originated from the RA. These findings indicate that the severity of fibrosis is important in the initiation of AF.

### Effects of PCL on Ca Transient

We analyzed the Ca transient duration at different PCLs. The results showed that the PCL did not affect the Ca transient duration (**Figure S5**).

### Effects of $CaCl_2$ Concentration on APD

The $APD_{80}$ of the RA and LA was 33.0±8.4 ms and 25.6±6.4 ms, respectively, at 1.8 mmol/L $Ca^{2+}$. After being exposed to low $Ca^{2+}$ Tyrode's solution (0.9 mmol/L $Ca^{2+}$), the $APD_{80}$ of the RA and LA significantly reduced to 26.9±5.1 ms and 22.9±4.4 ms, respectively (P=0.011 for RA, P=0.042 for LA).

### Comparison of Expression of SERCA2a and CSQ

Using western blot analysis, we compared the expression of Ca-handling proteins SERCA2a and CSQ between the Tx and Wt mice. As shown in **Figure S6** immunoblotting showed similar expression profiles for the Tx and Wt mice. The average expression ratio of the Tx to Wt mice was 0.85±0.19 (mean ± SD) for SERCA, (1.16±0.20) for CSQ in the atria, and 0.89±0.15 for SERCA and 0.95±0.14 for the CSQ in the ventricles. The differences were not statistically significant.

## References


S1. Brunner AM, Marquardt H, Malacko AR, Lioubin MN, Purchio AF. Site-directed mutagenesis of cysteine residues in the pro region of the transforming growth factor beta 1 precursor: Expression and characterization of mutant proteins. *J Biol Chem* 1989; **264:** 13660–13664.

S2. Nakajima H, Nakajima HO, Salcher O, Dittie AS, Dembowsky K, Jing S, et al. Atrial but not ventricular fibrosis in mice expressing a mutant transforming growth factor-$\beta_1$ transgene in the heart. *Circ Res* 2000; **86:** 571–579.

S3. Nygren A, Lomax AE, Giles WR. Heterogeneity of action potential durations in isolated mouse left and right atria recorded using voltage-sensitive dye mapping. *Am J Physiol Heart Circ Physiol* 2004; **287:** H2634–H2643.

S4. Glukhov AV, Flagg TP, Fedorov VV, Efimov IR, Nichols CG. Differential $K_{ATP}$ channel pharmacology in intact mouse heart. *J Mol Cell Cardiol* 2010; **48:** 152–160.

S5. Fedorov VV, Glukhov AV, Ambrosi CM, Kostecki G, Chang R, Janks D, et al. Effects of $K_{ATP}$ channel openers diazoxide and pinacidil in coronary-perfused atria and ventricles from failing and non-failing human hearts. *J Mol Cell Cardiol* 2011; **51:** 215–225.

S6. Wakimoto H, Maguire CT, Kovoor P, Hammer PE, Gehrmann J, Triedman JK, et al. Induction of atrial tachycardia and fibrillation in the mouse heart. *Cardiovasc Res* 2001; **50:** 463–473.

S7. Hartner A, Cordasic N, Rascher W, Hilgers KF. Deletion of the alpha8 integrin gene does not protect mice from myocardial fibrosis in doca hypertension. *Am J Hypertens* 2009; **22:** 92–99.

S8. Bray MA, Wikswo JP. Use of topological charge to determine filament location and dynamics in a numerical model of scroll wave activity. *IEEE Trans Biomed Eng* 2002; **49:** 1086–1093.

S9. Liu YB, Peter A, Lamp ST, Weiss JN, Chen PS, Lin SF. Spatiotemporal correlation between phase singularities and wavebreaks during ventricular fibrillation. *J Cardiovasc Electrophysiol* 2003; **14:** 1103–1109.

S10. Chou CC, Nihei M, Zhou S, Tan AY, Kawase A, Macias ES, et al. Intracellular calcium dynamics and anisotropic reentry in isolated canine pulmonary veins and left atrium. *Circulation* 2005; **111:** 2889–2297.

S11. Verheule S, Sato T, Everett T, Engle SK, Otten D, Rubart-von der LM, et al. Increased vulnerability to atrial fibrillation in transgenic mice with selective atrial fibrosis caused by overexpression of TGF-beta1. *Circ Res* 2004; **94:** 1458–1465.

S12. Nakajima H, Nakajima HO, Dembowsky K, Pasumarthi KB, Field LJ. Cardiomyocyte cell cycle activation ameliorates fibrosis in the atrium. *Circ Res* 2006; **98:** 141–148.